RESEARCH ARTICLE

Macromolecular Materials and Engineering
Open Access
www.mame-journal.de

The Use of Low-Quality Cotton-Derived Cellulose Films as Templates for In Situ Conductive Polymer Synthesis as Promising Biomaterials in Biomedical Applications

Sahin Demirci, Mehtap Sahiner, Shaida S. Rumi, Selin S. Suner, Noureddine Abidi, and Nurettin Sahiner**

Here, the use of cellulose films (CFs) produced from low-quality cotton is reported as a template for in situ synthesis of well-known conductive polymers, e.g., polyaniline (PANI) and polypyrrole (PPY) via oxidative polymerization. Three successive monomer loading/polymerization cycles of aniline (ANI) and pyrrole (PY) within CFs as PANI@CF or PPY@CF are carried out to increase the amount of conductive polymer content. The contact angle (CA) for three times ANI and PPY loaded and polymerized CFs as 3PANI@CF and 3PPY@CF are determined as 26.3±2.8 and 42.3±0.6 degrees, respectively. As the electrical conductivity is increased with increased number of conductive polymer synthesis within CF, the higher conductivity values, $3\times10^{-4}\pm8.1\times10^{-5}$ S.cm^{-1} and $2.1\times10^{-3}\pm5.8\times10^{-4}$ S.cm^{-1}, respectively are measured for 3PANI@CF and 3PPY@CF composites. It is found that PANI@CF composites are hemolytic, whereas PPY@CF composites are not at 1 mg mL^{-1} concentrations. All PPY@CF composites exhibit better biocompatibility than PANI@CF composites on L929 fibroblast cells with more than 70±8% viability at 1 mg of CF-based conductive polymer composites. Moreover, MIC and MBC values of 3PPY@CF composites for *Escherichia coli* (ATCC8739) and *Staphylococcus aureus* (ATCC6538) are determined as 2.5 and 5.0 mg.mL^{-1}, whereas these values are estimated as 5 and 10 mg.mL^{-1} for *Candida albicans* (ATCC10231).

1. Introduction

Fossil fuels dominate the materials currently used in various industries. The urgent concerns about climate change and plastic pollution have spurred the development of a bioeconomy, which involves substituting petroleum-based products with materials of biological origin or bio-based materials and with biodegradable alternatives.[1] An effective approach to address this issue is to utilize eco-friendly products. The benefits of ecologically friendly materials include non-toxicity, capacity to be sustained over time, and inherent biodegradability.[2] The need to establish a sustainable consumption has initiated exploration into utilizing natural cellulose as a substitute for non-renewable resources in many applications.[3–5] Cellulose has gained significant attention as a distinctive material due to its several inherent characteristics, including biodegradability, renewability, and widespread availability.[3,5,6] Cellulose is progressively recognized as a versatile source material for various

S. Demirci, S. S. Suner, N. Sahiner
Department of Chemistry
Faculty of Science
Canakkale Onsekiz Mart University Terzioglu Campus
Canakkale 17100, Turkey
E-mail: nsahiner@fgcu.edu

M. Sahiner
Department Bioengineering
Faculty of Engineering
Canakkale Onsekiz Mart University Terzioglu Campus
Canakkale 17100, Turkey

S. S. Rumi, N. Abidi
Fiber and Biopolymer Research Institute
Texas Tech University
1001 E Loop 289, Lubbock, TX 79403, USA
E-mail: Noureddine.abidi@ttu.edu

N. Sahiner
Department of Ophthalmology
Morsani College of Medicine
University of South Florida
Tampa, FL 33612, USA

N. Sahiner
Department of Bioengineering
Whitaker College of Engineering
Florida Gulf Coast University
U. A. Fort Myers, FL 33965, USA

The ORCID identification number(s) for the author(s) of this article can be found under https://doi.org/10.1002/mame.202400246

DOI: 10.1002/mame.202400246

applications, serving as a flexible biopolymer capable of producing hydrogels for absorbents, aerogels for insulation, membranes for filters, films for packaging, fibers for textiles and reinforcements.[1] Cellulose and its derivatives are commonly utilized in food packaging,[7] wound dressing,[8] and many other biomedical applications,[9,10] as cellulose based materials are readily biodegradable, and their degradation products are compatible with living organisms.

Some intriguing and remarkable organic materials, known as conducting polymers (CPs), are thought to possess special electrical and optical qualities analogous to those of inorganic semiconductors and metals. It is possible to synthesize CPs in an easy, adaptable, and economical manner.[11,12] Different approaches have been devised to adapt and adjust methods to prepare CPs to enable their integration and interaction with biological environments in biomedical applications such as biosensors and diagnostic devices.[13,14] These materials are continually sought for a number of biomedical uses, including bioengineering, regenerative medicine, and biosensors.[15–17] Some examples of common conductive polymers are polyacetylene (PA), polyaniline (PANI), polypyrrole (PPY), polythiophene (PTH), poly(paraphenylene) (PPP), poly(phenylenevinylene) (PPV), and polyfuran (PF).[11,18,19] Amongst them, the two conductive polymers most frequently employed are PANI,[20–22] and PPY.[23–25] Conductive polymers and their composites have a wide range of applications, including photo-catalysis,[26] anti-corrosion coatings,[27] biomedical tools,[10,21] energy storage materials,[28] and sensing devices.[29]

Most of the studies about cellulose based conductive polymer composite films generally involve bacterial cellulose and are quite costly.[30–32] The fact that bacterial cellulose is natural but developed in a laboratory environment makes the procedure quite costly. However, it is also very important to prepare cost-effective forms of currently reported cellulose/conductive polymer composites with similar or even superior properties at a low cost. The value of the study is increased by using CFs made from low-quality, unmarketable cotton fibers as a template for in situ conductive polymer synthesis to create intriguing viable biomaterials. Therefore, in this study, cellulose films (CFs) produced using naturally occurring cotton were used as templates for the synthesis of conductive polymers. The CFs prepared from low-quality cotton were used as templates for in situ synthesis of PANI and PPY conductive polymers. Structural and thermal characterization of the prepared CF-based conductive polymer composites, referred to as PANI@CF and PPY@CF, were performed to ascertain the relevant functional groups. The change in wettability properties of CF-based conductive polymer composites upon multiple ANI and PY monomer loading/polymerization cycles was investigated. The effect of multiple monomer loading/polymerization cycles on the conductivity of CF-based composites was also examined. Furthermore, blood compatibility of the CF-based materials was evaluated via hemolysis% and blood clotting index% (BCI) assays. Moreover, the cytotoxicity of CF-based composites on L929 fibroblast cells was investigated. The antimicrobial activity of CF-based conductive polymer composites was also analyzed against *Escherichia coli* ATCC8739 (*E. coli*), *Staphylococcus aureus* ATCC6538 (*S. aureus*), or *Candida albicans* ATCC10231 (*C. albicans*), microorganisms.

2. Results and Discussion

2.1. Structural Characterization of Conductive Polymer@CF Composites

Previously, Rumi et al. reported successful preparation of transparent and strong cellulose films (CFs) from low quality cotton fiber through dissolution, casting, regeneration, plasticization, and hot-pressing.[33] They exhibited improved stretchability, homogeneity, flexibility, and deformation recovery upon glycerol plasticization. According to the findings, plasticizing films containing 30% aqueous glycerol (w:v) had the highest deformation recovery, whereas adding more glycerol resulted in even weaker and more fragile films.[33] Therefore, in this investigation, cellulose film (CF) plasticized with 30% glycerol was used as a matrix for the in situ synthesis of conductive polymer. The schematic presentation of in situ conductive polymer synthesis within CF is given in **Figure 1**a,b.

It was noticed that the transparent CFs (size: 1.5 × 1.5 cm^2) changed colors upon placing into aniline (ANI) (slight yellow) and pyrrole (PY) (brownish) monomers. Upon polymerization of loaded ANI and PY monomers within CFs via oxidative polymerization technique,[34–36] as shown in Figure 1, a dark black coloration within CFs was observed for both composites. The in situ polymerization of ANI within CF pieces was carried out in APS/HCl solution.[37] In contrast, in situ polymerization of PPY within CF pieces was carried out in aqueous $FeCl_3$ solution.[38] Several studies have reported that the radical coupling mechanism occurs in the chemical polymerization of both ANI and PY.[39–43] Thus, the visual dark black appearance (Figure 1) of the resultant composite confirmed successful synthesis of conductive polymer within CF matrixes. Furthermore, the in situ synthesis of PANI and PPY conductive polymers was repeated up to three times in order to enhance the amount of conductive polymer within CF matrices. Therefore, to increase the amount of conductive polymer within CFs matrices, the in situ synthesis of PANI and PPY conductive polymers within CF pieces were carried out up to three times, repetitively. For this purpose, the prepared 1PANI@CF and 1PPY@CF pieces were placed in ANI and PY monomers to load more of the related monomers into corresponding CFs by mixing at 250 rpm for 12 h again. Next, the excess amount of monomer from the surface of ANI and PY loaded 1PANI@CF and 1PPY@CF pieces were gently removed with a paper tissue. Then, the ANI and PY loaded 1PANI@CF and 1PPY@CF pieces were placed into initiators solutions, which is APS:HCl solution for polymerization of ANI, and aqueous $FeCl_3$ solution for polymerization of PY within 1PANI@CF and 1PPY@CF pieces, respectively. For the third loading/polymerization cycles of ANI and PY within CFs, the same procedure was applied to 2PANI@CF and 2PPY@CF pieces, as mentioned above. The mechanical properties of bare CFs have been studied in detail by Rumi et al.[33] It was reported that the tensile strength values of glycerol-free CFs were much higher than the glycerol-containing CF forms, and their elongation values were lower. However, it was stated that glycerol-free CFs had higher young modulus values than the glycerol-containing forms. As the mechanical properties of the PANI@CF and PPY@CF composites prepared in this study were compared with bare CF, it was observed that the CF composites containing

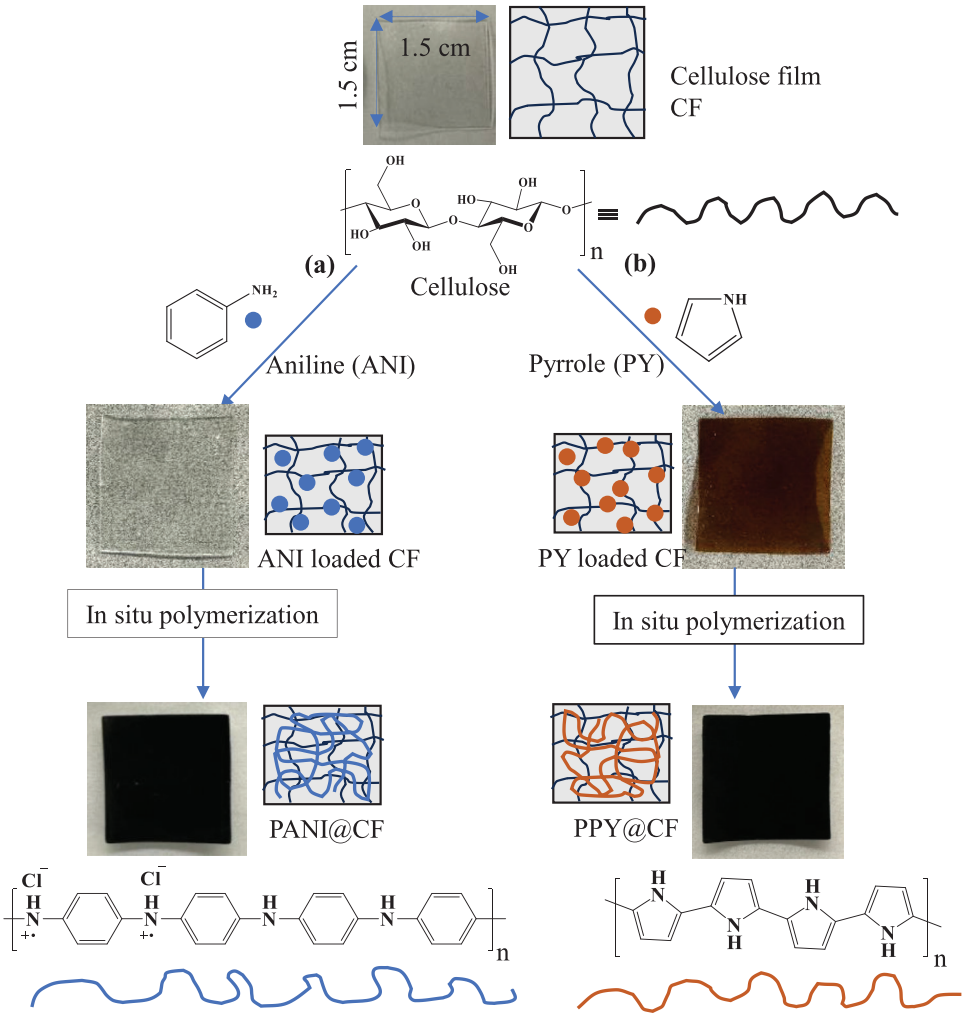

Figure 1. The schematic depiction of in situ conductive polymers a) PANI, and b) PPY within CFs as PANI@CF and PPY@CF.

conductive polymer were found much more brittle than bare CF when dried at 24 h at 50 °C but kept their elastic properties when kept moist.

FT−IR spectra of CFs, PANI@CFs, and PPY@CFs were collected to confirm the in situ synthesis of the conductive polymer in the matrix. Also, the FT-IR spectra after the multiple monomers loading and then in situ conductive polymer synthesis within CFs, for PANI@CFs, and PPY@CFs were recorded and shown in **Figure 2**. The most noticeable standing out peaks in FT-IR spectra of CFs were broad −OH stretching vibrations at 3287 cm^{-1}, −OH bending at 1655 cm^{-1}, and $-CH_2$ scissoring at 1459 cm^{-1}, C−H bending at 1314 cm^{-1}, asymmetric ring stretching at 1112 cm^{-1}, C−O stretching at 1032 cm^{-1}, and beta linkage of cellulose at 853 cm^{-1}, respectively.[33] On the other hand, the peaks at 2994 and 2881 cm^{-1} assigned to −CH stretching from glycerol were also observed.[33] The FT-IR spectrum of 1PANI@CF composite exhibited the distinctive peak for PANI at 1580 cm^{-1} associated with benzenoic–quinonic nitrogen vibration[44,45] along with CF peaks (Figure 2a). In the FT-IR spectra of 2PANI@CF and 3PANI@CF composites, all of the peaks found for neat CFs almost disappeared, with the exception of the peaks arising from cellulose between 1100−800 cm^{-1}. Nevertheless, the intensity of the peak at 1580 cm^{-1} increased as the number of in situ PANI synthesis increased. The spectra also showed the appearance of additional vibration bands that were characteristics of PANI, including aromatic C–C peaks at 1478 cm^{-1}, aromatic amine peaks at 1285 cm^{-1}, and C–N–C peaks at 1146 cm^{-1}.[44–46] Besides, the FT-IR spectra of PPY@CFs displayed in Figure 2b revealed the disappearance of almost all peaks observed in the FT-IR spectra of neat CFs, such as the peaks originating from cellulose in the range of 1100−800 cm^{-1}, even after the first synthesis of PPY within CFs. Consequently, there newly appeared peaks with higher intensity as the number of polymerization cycles increased. These included −C = C peak at 1701 cm^{-1}, fundamental PPY ring vibration at 1539 cm^{-1}, N–C stretching vibrations at 1288 cm^{-1}, and out-of-plane bending of C−H at 976 cm^{-1}, deriving from PPY.[46] These spectroscopic changes related to respective conductive polymers confirmed their effective synthesis within the matrix and the increase of their quantity with each synthesis cycle.

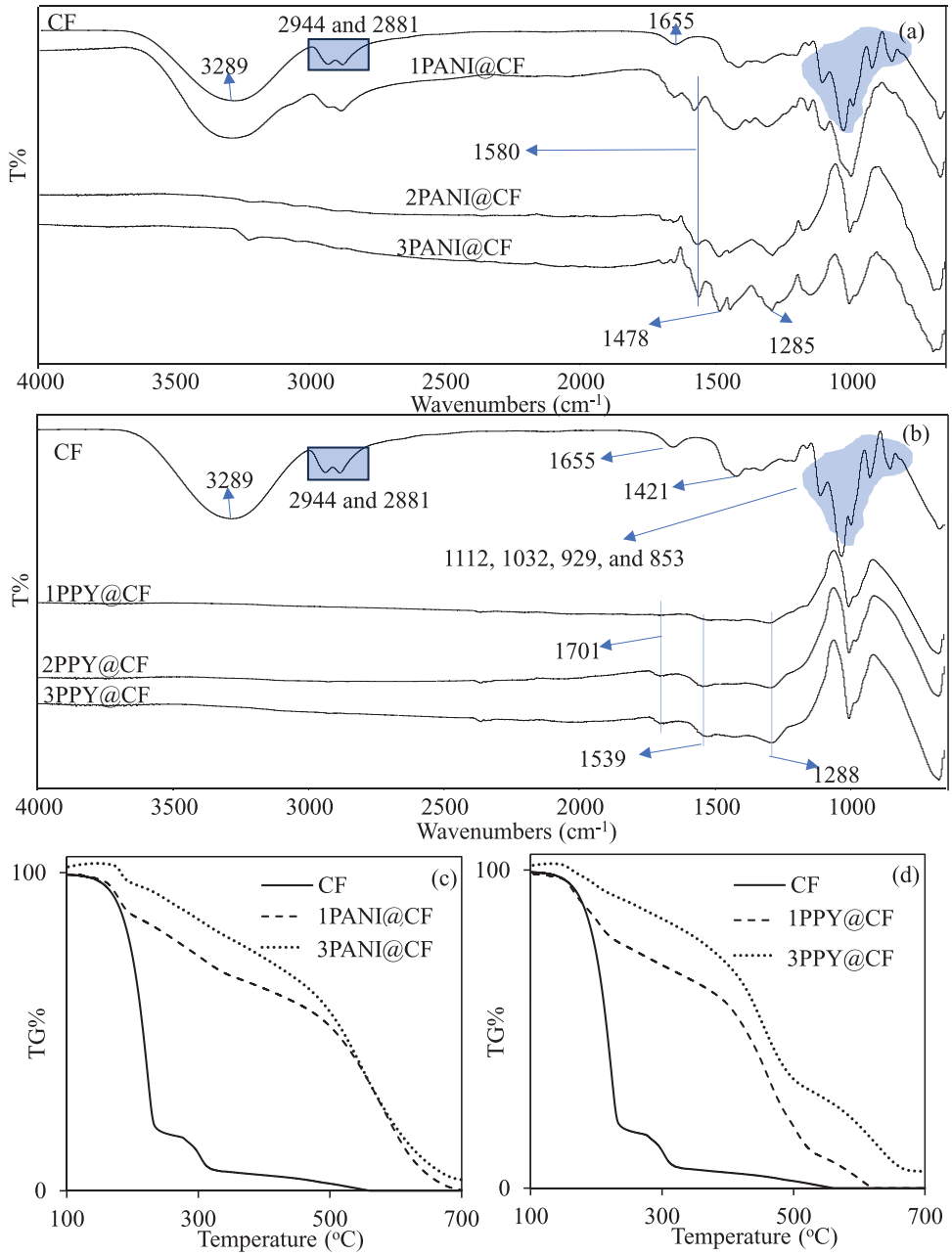

Figure 2. The FT-IR spectra of a) PANI@CF, b) PPY@CF, and TGA thermograms of c) PANI@CF and d) PPY@CF composites.

Furthermore, the thermal degradation profiles of bare CF, PANI@CF, and PPY@CF are illustrated in Figure 2c,d, respectively. A significant weight loss was observed for CF between 150–240 °C, accounting for an 80.3% reduction, attributed to glycerol decomposition.[33] Additionally, the observed cumulative weight loss of 92.8% between 270–315 °C was related to the decomposition of cellulose.[33] The weight of 1PANI@CF decreased by 12.7% between 165–195 °C (Figure 2c), an indication of a lesser amount of glycerol content in the composite due to the presence of PANI. In addition, the weight loss in the range of 200–460 °C and 465–650 °C, corresponding to 45.3% and 95.3% reduction, could be ascribed to the decomposition of cellulose and PANI, respectively. The 3PANI@CF[d] exhibited a similar thermal degradation profile to the 1PANI@CF, the cumulative weight losses values at 180–195, 200–465, 470–650 °C were determined as 2.9, 39.6, and 91.5%, respectively.

Also, the thermal degradation behavior of CFs and its' situ prepared PPY composites were compared, and the corresponding results were illustrated in Figure 2d. It was also noted that the in situ preparation of PPY within CFs caused removal of glycerol from structure pertaining to decrease in weight losses at 160–230 °C range with 22.7, and 8.4% weight losses for 1PPY@CF, and 3PPY@CF respectively. The weight loss in 200–460 °C range was determined as 42.2, and 30.9% for 1PPY@CF, and

Table 1. The amount of in situ synthesized conductive polymers within CFs upon multiple monomer loading/polymerization cycles.

Weight of bare CF [mg] *	CF-based composites	Amount of in situ synthesized conductive polymers within CFs [mg g^{-1}] / (mmoles)**		
		Numbers of conductive polymer loading		
		1	2	3
23.2±1.9	PANI	176.6±10.2 / 1.9±0.1	355.7±26.8 / 3.8±0.3	724.8±99.7 / 7.8±1.1
	PPY	231.1±39.6 / 3.4±0.6	595.1±62.7 / 8.9±0.9	833.8±25.3 / 12.4±0.4

*The weight of CFs was measured after washing in water for 24 h. **mmoles were calculated according to repeating units of related conductive polymers.

3PPY@CF, respectively. The cumulative weight loss at 700 °C was >99, and 94.7% for 1PPY@CF, and 3PPY@CF correspondingly. It can be presumed that after three loading/polymerization cycles of PANI and PPY within CFs, the amount of glycerol is decreased due the replacement of it with ANI and/or PY because of the increased amount of PANI and PPY within CF upon their individual polymerizations were observed. These findings indicated that PANI@CF and PPY@CF composites exhibited greater thermal stability compared to CF, as the presence of PANI and PPYs in the CFs cellulose afforded excellent thermal degradation profile due to the interactions between the guest polymers (PANI or PP) and the host, CF.[47] The thermal stability of bare CF was much less upon comparison to PANI@CF and PPY@CF composites. This can be attributed to the increased inter- and intra-molecular interaction of CF with PANI and PPY synthesized within CF.[48] Consequently, a higher extent of energy is necessary to break down the interaction of PANI and PPY with CF chains in comparison to the bare CF.[49,50]

The amounts of PANI and PPY synthesized within CF pieces upon in situ polymerizations were determined gravimetrically following each loading/polymerization cycle, and the corresponding results are summarized in **Table 1**. The FT-IR analysis indicated the replacement of glycerol from the CF structure even during the initial monomer loading/polymerization procedure. To quantify the amount of PANI and PPY synthesized with or in situ in CFs, five pieces of CF (1.5 × 1.5 cm^2) were washed in 50 mL of water for 24 h, and after drying, their weight was measured as the control. The digital camera images of washed and dried CF and conductive polymer@CF composites are shown in Figure S1 (Supporting Information). It was noticed that the CFs wrinkled, visibly hardened, and became more brittle after washing and drying.

The average weight of five pieces of CF was 93.2±8.1 mg, which decreased to 23.2±1.9 mg after 24 h of washing in water. This reduction indicated the removal of 75.1±2.0% of glycerol from the structure, a finding consistent with the TGA results presented in Figure 2b. The quantities of PANI in CF after 1, 2, and 3 cycles of monomer loading/polymerization were measured as 176.6±10.2, 355.7±26.8, and 724.8±99.7 mg g^{-1}, respectively, illustrating an increase in polymer content within the CF with each successive cycle. Likewise, the quantities of PPY in 1PPY@CF, 2PPY@CF, and 3PPY@CF were determined to be 231.1±39.6, 595.1±62.7, and 833.8±25.3 mg g^{-1}, respectively. This demonstrated that the amount of in situ synthesized PANI increased from 1.9±0.1 to 7.8±1.1 mmoles (based on repeating unit of PANI) through successive monomer loading and polymerization cycles, while the amount of in situ synthesized PPYs within CFs increased from 3.4±0.6 to 12.4±04 mmoles (based on repeating unit of PPY).

2.2. The Wettability Properties of Conductive Polymer@CF Composites

The wetting ability of CFs and conductive polymer@CF composites were assessed through contact angle (CA) measurements. A droplet of 10 µL of DI water was deposited on the samples. As per our previous study, the contact angle of water on plasticized CFs was <15°, while for non-plasticized CF was >80°. The decrease in CA was attributed to the inherent hydrophilicity of glycerol.[33] The CA value of 11.6±0.4 ° for CF was determined in this study after washing and drying whereas the contact angle value was measured as 90.6±3.7° before washing and drying and corresponding values compared in **Figure 3a**. The CA values were determined in two different states. The first state, referred to as "as is", involved measuring the contact angles of composites immediately after the completion of the in situ conductive polymer synthesis process. Water from the sample surface was wiped off before taking the measurement. In the second state, the composites were in their dried forms. Bare CF ("as is") was washed and dried to make a comparison of CA with composites in the second state. The CA of dried CF increased to 90.6±3.7° from 11.6±0.4° due to the loss of hydrophilic glycerol. The measured CA values ("as is" state) for 1PANI@CF, 2PANI@CF, and 3PANI@CF composites were calculated as 42.9±0.6, 39.5±1.9, and 26.3±2.8°, respectively, which were at least 2-fold higher than bare CF (11.6±0.4°). The CA of PANI@CF composites after washing and drying, increased as well to 86.5±1.6, 65.5±1.3, and 38.7±08 ° for consecutive cycle of polymerization, although remaining lower than bare CF. The images of water droplets on CF and PANI@CF composites in both states were given in Figure S2 (Supporting Information). In both instances, it was observed that wettability of the composites CFs was increased with the increase in PANI content. This phenomenon can be attributed to emeraldine salt form of PANI which was transformed into during polymerization in the presence of HCl. PANI is relatively hydrophobic in emeraldine base form, and its water CA value is between 94–84°.[51,52] Also, the emeraldine salt form of PANI can occurred in the presence of other acids such as HNO_3, etc. shows lower contact angles.[53,54] Another parameter surface free energy (SFE) values for CF based composites were also calculated. There are various SFE calculation methods and techniques.[55] Here, Owen-Wendt-Rabel-Kaelble (OWRK) model (Equation 1) was employed to calculate the SFE of prepared materials using water and diiodomethane as hydrophilic and hydrophobic

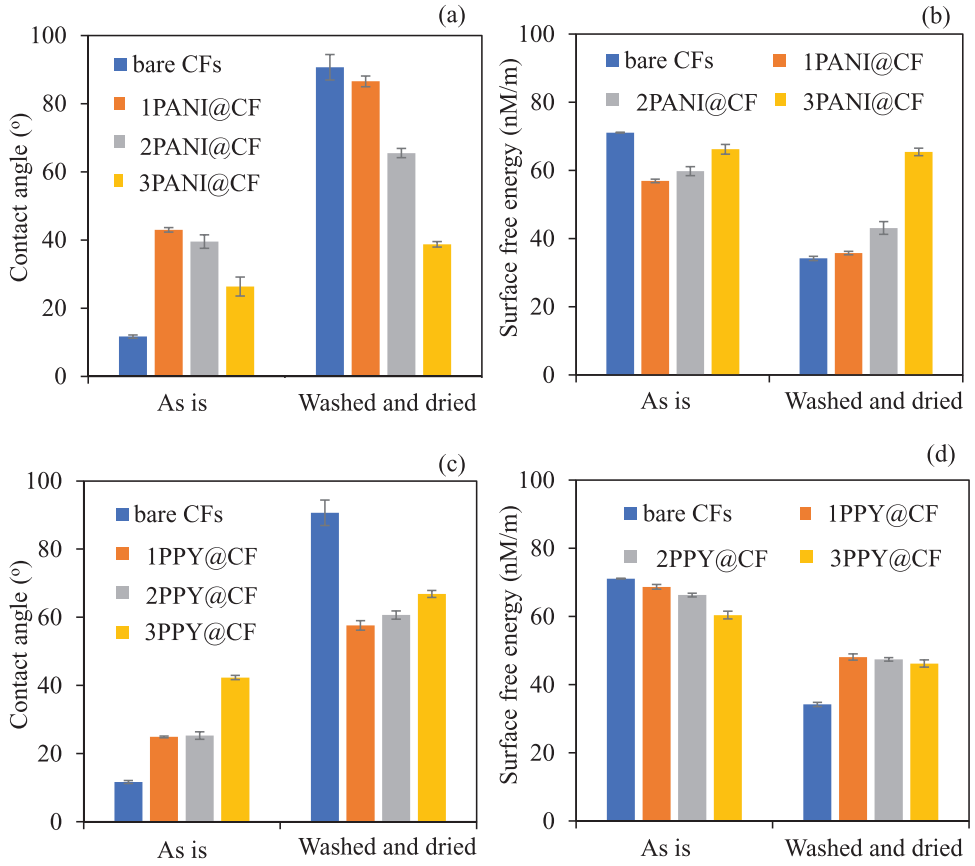

Figure 3. Changes on a) CA, and b) surface free energy values for PANI@CF and the changes on c) CA, and d) surface free energy values for PPY@CF composites after multiple monomer loading/polymerization cycles.

solvents, respectively.[56] The surface free energy is calculated using the material's dispersive and polar force components.

$$\left(\gamma_{sv}^{d}\gamma_{lv}^{d}\right)^{1/2} + \left(\gamma_{sv}^{p}\gamma_{lv}^{p}\right)^{1/2} = 0.5 + \gamma_{lv}\left(1 + \cos\left(\theta_{\gamma}\right)\right) \quad (1)$$

where γ_{sv} and γ_{lv} are the surface tensions of the solids and liquids, respectively; superscripts "d" and "p" are the dispersive and polar force components; and, finally, θ_{γ} is the contact angle of the liquid. Previously, it was shown that utilizing water and diiodomethane yields accurate results.[57] Therefore, DI water and diiodomethane were utilized to calculate the dispersive and polar force components of CF-based composites. The SFE values for CF in "as is" form was 71.1±0.1 mN m^{-1} (CA is 11.6±0.4°), whereas it was 56.9±0.5, 59.8±1.3, 66.2±1.4 mN m^{-1} for PANI@CF 1PANI@CF, 2PANI@CF, and 3PANI@CF, respectively, as given in Figure 3b. On the other hand, the surface free energy (SFE) for washed and dried CF was 34.2±0.6 mN m^{-1}, while SFE was 35.8±0.5, 43.1±1.8, 65.4±1.1 mN m^{-1} for dried PANI@CF 1PANI@CF, 2PANI@CF, and 3PANI@CF, respectively. The calculated SFE values agree with the calculated CA values for each related CF-based structure prepared in this study.

In contrast, it was found that monomer loading/polymerization cycle had a positive impact on increasing CA of PPY@CF composites as illustrated in Figure 3c. The CA values for 1PPY@CF, 2PPY@CF, and 3PPY@CF composites increased to 57.6±1.4, 60.7±1.2, and 66.8±1.0° in the second state from 24.9±0.2, 25.3±1.1, and 42.3±0.6°, respectively. The photographs of water droplet on PPY@CF composites are given in Figure S3 (Supporting Information). The CA of composites increased with the increased amount of PPY in the matrix. Similarly, a study by Fraser and van Zyl also reported the increase of CA from 35.8° to 48.5° with an increase of polymerization time from 50 min to 20 h for the bacterial cellulose-PPY composites.[58] It was also reported that covering individual cellulose fibers with a continuous PPY coating led to decreased capillary forces, thereby enhancing the contact angle between water and the composite fibers.[59] Additionally, the presence of PPY hindered the formation of hydrogen bonds between the individual fibers while they were in a dry state.[59] The SFE values for PPY@CF composites were found to decrease with the increasing value of CA after multiple PPY loading/polymerization cycles (Figure 3d). The "as is" SFE value for 1PPY@CF, 2PPY@CF, and 3PPY@CF composites were calculated as 68.7±0.7, 66.3±0.5, and 60.4±1.1 mN m^{-1}, respectively. These values decreased to 8.1±0.9, 47.4±0.5, and 46.2±1.1 mN m^{-1}, respectively, in the subsequent state.

In summary, the in situ synthesis of conductive polymer within CFs directly affected their wettability properties. The presence of conductive polymers provided tunable hydrophilicity of the composites depending on the specific monomers used and the quantity of polymer present in the substrate. Various studies have documented the ability to manipulate the wetting properties through applied voltages.[60–65] The prepared

conductive polymer@CF composites could be potentially used not only in sensors but also in providing controlled hydrophilicity/hydrophobicity to render additional functionalities.

2.3. Electrical Conductivity Comparisons of Conductive Polymer@CF Composites

Commercial application of conductive polymers presents several challenges because of their high cost, poor processability, and lack of repeatability. However, these materials are appealing owing to their unconventional properties, such as the ability for chemical modification, optical capabilities, and potential use in energy and sensor applications. They are considered cutting-edge materials with a variety of potential uses.[11,12,19,66,67] The unique electrical conductivity of these organic polymers is due to the existence of conjugated bonds and linkages and/or heteroatoms with unshared electron pairs. During polymerization, the oxidation of monomers, either chemically or electrochemically, generates the conjugated backbone of conductive polymers. The conjugation process occurs in two distinct phases: first, the monomers undergo oxidation, followed by the polymerization and the oxidation of the polymers. This oxidation creates a space for the incorporation of negatively charged dopants or counter ions, such as chloride.[68] The dopant concentration in polymers is usually below one per polymer unit, often ranging from 0.3 to 0.5. This concentration is strongly influenced by the proximity of the polymer units along the polymer chain. In supercapacitor devices, PANI and PPY are commonly utilized as conductive polymers.[69] Polarons and bipolarons play a crucial role in realizing the conductivity and electrical conduction along the polymer backbone in the presence of an electric field. The widely recognized conduction process entails the movement of electric charge along the chains of conductive electroactive polymers, as well as the transfer of carriers across chains through hopping. In this study, the electrical conductivities of prepared conductive polymer@CF composites were also studied. The details and the depiction of the experimental arrangement used to test the conductivity of CF, PANI@CF, and PPY@CF composites using I-V curves were conducted in accordance with the literature.[46,70] The electrodes of the electrometer were in contact with the CFs, with conductive carbon tapes connected to both the top and bottom sides. The I-V curves were recorded via a computer. **Figure** 4a,b depict the comparisons of I-V curves of bare CFs with PANI@CFs and PPY@CFs composites, respectively. The conductivities of the bare CF, PANI@CF, and PPY@CF composites were calculated using Equation 1 and 2 and are summarized in Figure 4c.

$$V = I\,x\,R \tag{2}$$

$$\sigma = \left(\frac{1}{R}\right) x \left(\frac{I}{A}\right) \tag{3}$$

where, "V" is voltage, "I" is current, "R" is the bulk resistance, "σ" is conductivity, "1/R" is resistivity, "l" is the thickness and "A" is the cross-sectional area of the sample. The conductivity of bare CFs, as shown in Figure 4c, was determined to be $7.0\times10^{-8}\pm1.0\times10^{-8}$ S.cm^{-1}. On the other hand, the conductivity value of bare CF increased to $3.2\times10^{-6}\pm9.4\times10^{-7}$ S.cm^{-1} with the presence of in situ prepared PANI for once which is equal to almost 50-fold increase in conductivity with respect to bare CFs. Moreover, the multiple ANI loading/polymerization cycles to increase amount of in situ prepared PANI within CF resulted in a significant increase in conductivity.

Accordingly, the conductivity values for 2PANI@CF and 3PANI@CF composites were calculated as $7.6\times10^{-5}\pm9.3\times10^{-6}$ S.cm^{-1} and $2.3\times10^{-4}\pm8.1\times10^{-5}$ S.cm^{-1}, respectively. The calculated conductivity values for 2PANI@CF and 3PANI@CF composites were 1.1K (K = 1000) and 3.3K times higher than the conductivity value of bare CFs, respectively. On the other hand, the conductivity of 1PPY@CF composites was determined as $1.3\times10^{-3}\pm7.9\times10^{-4}$ S.cm^{-1} which is almost 20K times higher than conductivity of bare CFs. Similarly, the conductivity of PP@CF composites was increased with multiple pyrrole loading/polymerization cycles to $1.7\times10^{-3}\pm7.0\times10^{-4}$, and $2.1\times10^{-3}\pm5.8\times10^{-4}$ S.cm^{-1} for 2PPY@CF, and 3PPY@CF composites, respectively. This shows that the calculated conductivity values for 2PPY@CF and 3PPY@CF composites are 24K and 30K higher than the conductivity of bare CF, respectively. The increase on conductivity via multiple monomer (ANI or PY) loading/polymerization cycles can be explained with increased amount of in situ synthesized conductive polymers, as given in Table 1. The significant improvements in the conductivity of conductive polymers in CF as conductive polymer@CF composites explicitly demonstrates the successful synthesis of conductive polymers within bare CF matrix by means of multiple monomer loading/polymerization cycles of ANI and PY to CFs resulted in higher conductivity values. The reported conductivities range for PANI systems is between 10^{-10}–10^{1},[71] whereas it is 10^{-7}–10^{3} for PPY systems.[72] The observing lower conductivities than bare forms of related conductive polymers can be explained with the effect of CF templates. The conductivity values for 3PANI@CF and 3PPY@CF composites are comparable to conductive polymer composites with similar architectures reported in different other studies.[58,73–77] For instance, carboxymethyl cellulose-conductive polymer composite cryogels, CMC-PANI, and CMC-PPY, exhibited conductivities of 4.6×10^{-4} and 5.0×10^{-5} S cm^{-1}, respectively.[73] Additionally, bacterial cellulose, methyl cellulose, hydroxypropyl methyl cellulose, and carboxymethyl cellulose PANI composite fabrics displayed conductivities of 199×10^{-2}, 2.84×10^{-2}, 2.08×10^{-2}, and 0.96×10^{-2} S cm^{-1} respectively.[75] The cellulose nanofiber-PPY composite had a conductivity of 2×10^{-2} S cm^{-1}.[74] Moreover, bacterial cellulose-PANI blend showed a conductivity of 1.4×10^{-1} S cm^{-1},[76] while another study reported a remarkably high conductivity of 1.94×10^{0} S cm^{-1} for bacterial cellulose-PPY composite.[58] Various formulation of cellulose are reported for conductive material preparation, e.g., the coating of cellulosic paper with PANI/cellulose nanocrystal composites also afforded very high conductivity, 4×10^{0} S cm^{-1}.[77]

2.4. Biocompatibilities of Conductive Polymer@CF Composites

Hemocompatibility and biocompatibility of materials are the most essential requirements for determining their potential use in biomedical applications. Therefore, the hemocompatibility of prepared PANI@CF and PPY@CF composites was investigated via hemolysis and BCI assays. In **Figure** 5a, the hemolysis%

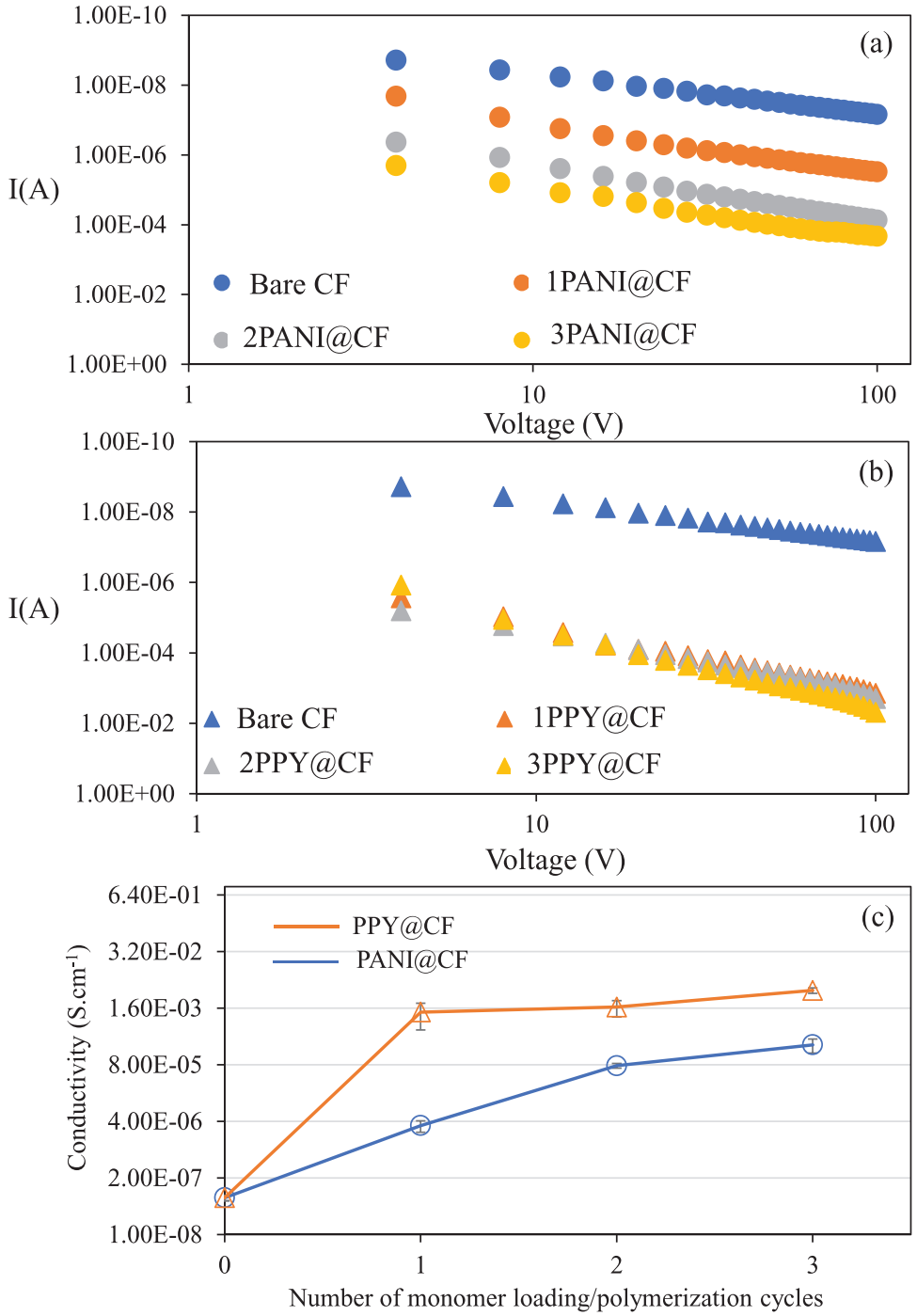

Figure 4. The ohmic region of I–V curves for a) PANI@CF, b) PANI@CF composites, and c) the comparison of the conductivity values of PANI@CF and PANI@CF composites.

results for bare CF, PANI@CF, and PPY@CF composites are compared. According to the American Society for Testing and Materials (ASTM), hemolysis below 5% is referred to as non-toxic, up to 10% is regarded as minor, and more than 10% is considered significant.[78] Hemolysis is defined as the rupture or alteration of the red blood cell membrane, leading to the release of hemoglobin.[79] The hemolysis% values for bare CF were found to be 0.13±0.12% at 1 mg mL^{-1} concentrations, which indicated that bare CFs are nonhemolytic. However, the hemolysis ratio increased due to the in situ synthesis of PANI, and at 1 mg mL^{-1} concentrations, the 1PANI@CF, 2PANI@CF, and 3PANI@CF composites showed significant hemolysis with values of 37.6±2.8, 29.2±4.2, and 19.7±2.9%, respectively. Conversely, the hemolysis% values of the 1PPY@CF, 2PPY@CF, and

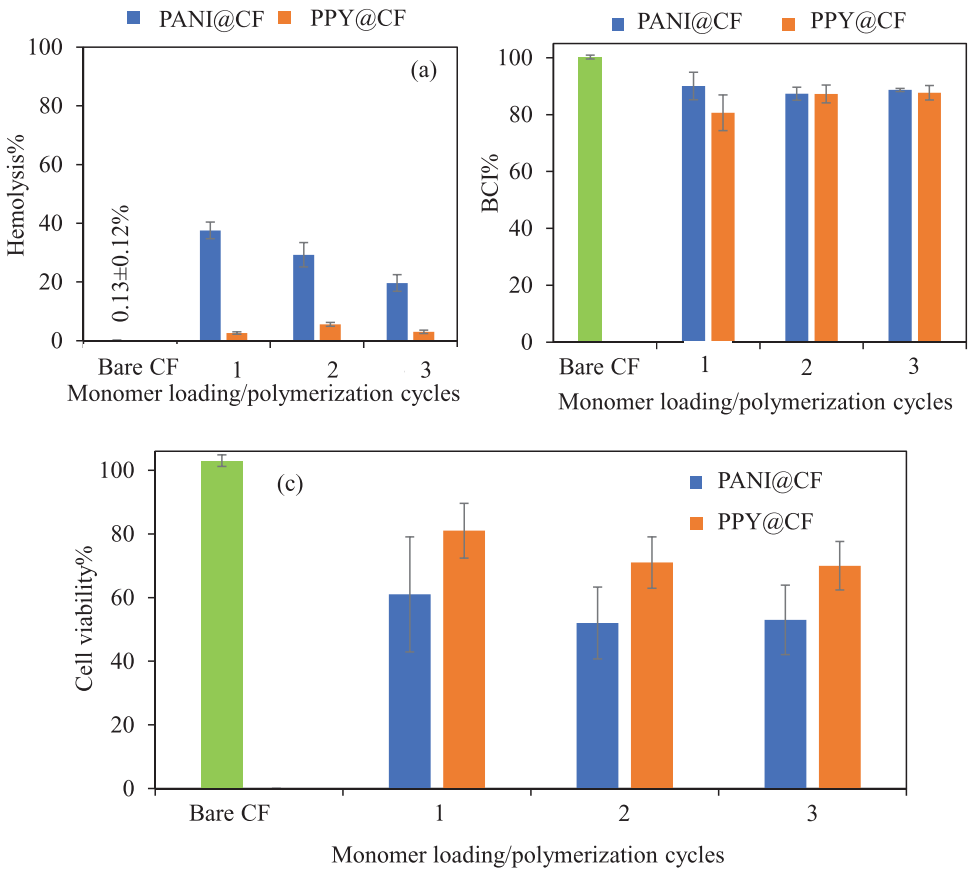

Figure 5. Blood compatibility of CF-based conductive polymer composites via a) hemolysis% assay, b) blood coagulation assay at 1 mg mL^{-1} concentration, and c) cytotoxicity of conductive polymer@CF composites on L929 fibroblast cell.

3PPY@CF composites were 3.0±0.6%, 5.5±0.7, and 2.6±0.4, respectively, implying a non-hemolytic nature. As PPY was introduced into an animal's body, no carcinogenic effects, allergies, or hemolysis of red blood cells were reported.[80] It was also reported that PPY-polyvinyl alcohol composites showed great hemocompatibility with non-hemolytic nature.[81] So, it is apparent that PPY-based composites are non-hemolytic materials. Another test that is widely used to evaluate the compatibility of materials with blood is the blood clotting index (BCI). Clotting agents play a crucial role in controlling bleeding, thus making them vital components of wound dressing materials. BCI is particularly important in assessing the efficacy of any clotting agents, with lower values indicating superior coagulation effects. The effect of bare CF, PANI@CF, and PPY@CF composites on the blood coagulation process is shown in Figure 5b. It was observed that the bare CFs had no effect on coagulation, while PANI@CF and PPY@CF composites exerted a modest impact with 90% BCI. Depending on the specific needs, such as excessive bleeding or the need to prevent blood loss, clotting agents may be necessary to stop bleeding in certain applications including surgery or accidents. These agents can also be valuable for wound dressing materials. However, it is often imperative to avoid any disruption to the blood coagulation systems when using materials in biological applications. In general, BCI is around 100% considered no interaction with the blood clothing mechanisms. It was observed that the bare CFs did not affect the blood clotting mechanism with 100.2±0.7% BCI value. On the other hand, the prepared PANI@CF and PPY@CF composites exhibit slight effect on blood coagulation mechanism about 90% BCI values.

Furthermore, the cytotoxicity of PANI@CF and PPY@CF composites was compared with neat CF on L929 fibroblast cells, and the results are shown in Figure 5c. The cell viability% at 1 mg of CF was determined as 103±2%, while the cell viability of 1PANI@CF, 2PANI@CF, and 3PANI@CF composites was determined as 61.2, 52.1, and 53.1%, respectively. The toxicity of PANI@CF composites increased due to the increased PANI content in CFs. However, the results for 1 mg PPY@CF composites showed moderate toxicity on L929 fibroblast cell.[82] Nevertheless, the cell viability% of 1PPY@CF, 2PPY@CF, and 3PPY@CF composites against L929 fibroblast cells at the same concentration was found to be 81±9, 71±8, and 70±8%, respectively. While 1PPY@CF composites were within the limit of non-toxicity, both 2PPY@CF and 3PPY@CF composites revealed modest toxicity toward L929 fibroblast cells. It is apparent that the types of polymers (PANI versus PPY) have some impact on the cytotoxicity of the composite materials. However, other parameters such as the addition of different oxidizing agents, e.g., whether of chemical or biological origin, or the amounts of doping agents, or

Table 2. Antimicrobial activities of CF-based conductive polymer composites against gram-negative *E. coli*, gram-positive *S. aureus*, and a fungus, *C. albicans*.

Materials	*E. coli*		*S. aureus*		*C. albicans*	
	MIC [mg mL^{-1}]	MBC [mg mL^{-1}]	MIC [mg mL^{-1}]	MBC [mg mL^{-1}]	MIC [mg mL^{-1}]	MBC [mg mL^{-1}]
CF	*N.D.	N.D.	N.D.	N.D.	N.D.	N.D.
3PANI@CF	N.D.	N.D.	N.D.	N.D.	N.D.	N.D.
3PANI@CF^{+}	10	N.D.	10	N.D.	10	N.D.
3PPY@CF	2.5	10	2.5	10	5	10
3PPY@CF^{+}	2.5	10	2.5	10	5	10

even or type of cell lines, should be taken into consideration. The cytotoxic effects of PANI-based composites on various cell lines vary depending on factors such as PANIs's size, shape, oxidation state, and impurity level.[21] PANI exhibits higher cytotoxicity in its emeraldine salt form compared to its emeraldine base form.[83] However, a mouse embryonic fibroblast cell line (NIH/3T3) or embryonic stem cells (ES R1 (ESc)) did not show any cytotoxicity when the concentration of emeraldine salt was kept below 2.5 µg mL^{-1}.[84] Nevertheless, the cytotoxicity of PANI on mouse embryonic fibroblast cells can be influenced by an acid dopant. Zhang et al. demonstrated that the cytotoxicity increased in the following order: PANI-phosphoric acid < PANI-hydrochloric acid < PANI-sulfuric acid < PANI-methanesulfonic acid < PANI-nitric acid. Even at 20 ppm doses, the most common HCl-doped PANI did not appear to be cytotoxic.[85] A different investigation indicated that PPY nanoparticles demonstrated non-toxic behavior at a concentration of 100 µg mL^{-1} when tested on fibroblast (L929), colorectal adenocarcinoma (HT29), and pancreatic acinar (266−6) cells.[86] Conversely, PPY particles synthesized via oxidative polymerization in the presence of sodium dodecyl sulfate (SDS) exhibited cytotoxic effects at concentrations exceeding 19.4 µg mL^{-1} on primary mouse embryonic fibroblasts (MEF), mouse hepatoma (MH-22A) cells, and human T lymphocyte Jurkat cells.[87] Therefore, it is essential to consider various parameters when utilizing conductive polymer-containing composite materials for in vivo biomedical applications.

2.5. Antimicrobial Activities of Conductive Polymer@CF Composites

Two of the important applications of cellulose-based materials are in packaging,[88–90] and wound dressing.[91–93] Given this, it is crucial for cellulose based materials to possess some level of antimicrobial properties against various microorganisms. Therefore, the antimicrobial effectiveness of the conductive polymer@CF composites was evaluated against gram-negative *E. coli*, gram-positive *S. aureus*, and a fungus, *C. albicans*, and the results are summarized in **Table 2**.

As anticipated, bare CF displayed no antimicrobial effect up to a concentration of 10 mg mL^{-1}, consistent with prior studies.[94–96] Similarly, no antimicrobial activity was observed for the 3PANI@CF composites at the same concentration. However, the 3PPY@CF composites exhibited some antibacterial activity against three microorganisms. Specifically, the MIC value for *E. coli* and *S. aureus* bacteria was 2.5 mg mL^{-1}, with MBC values of 10 mg mL^{-1}. Conversely, the MIC and MBC values against *C. albicans* were 5 mg mL^{-1} and 10 mg mL^{-1}, respectively. To assess the potential enhancement of antimicrobial activity following the protonation of amine-containing polymers, the conductive polymer@CF composites were treated with 25 mL of 1 M HCl. For the 3PANI@CF^{+} composites, the MIC value against *E. coli*, *S. aureus* bacteria, and *C. albicans* fungus was determined to be 10 mg mL^{-1}. In contrast, there were no changes observed in the antimicrobial effect of the 3PPY@CF composites after protonation. The MIC value remained at 2.5 mg mL^{-1} for *E. coli* and *S. aureus* bacteria, and 5 mg mL^{-1} for *C. albicans*, with corresponding MBC values of 10 mg mL^{-1}. Accordingly, for 3PPY@CF composites, the MIC value against *E. coli* and *S. aureus* bacteria was found to be 2.5 mg mL^{-1}, and the MBC values were found to be 10 mg mL^{-1}. On the other hand, MIC, and MBC values for 3PPY@CF composites against *C. albicans* were determined as 5 and 10 mg mL^{-1}, respectively. These results are comparable with some previously reported in different literature.[94–100] For instance, PANI/Cell composite displayed slight antimicrobial activity at 10 mg mL^{-1} concentrations with 27.7±0.5, 32.9±0.7, and 39.1±0.6% inhibitions against *E. coli*, *B.subtilis*, and *C. albicans*, respectively.[96] Another study reported MIC values of 2.5 mg mL^{-1} and 1.25 mg mL^{-1} for cellulose/PANI composites against *E. coli* and *S. aureus*, respectively[99] Although PANI may be considered a good antibacterial material, it has also been stated that cellulose/PANI composites have significant potency to eliminate pathogens, but are only capable of significantly reducing bacterial loads,[101] due to the presence of cellulose that does not possess any antibacterial properties. However, it has also been reported that ternary nanofillers such as silver nanoparticles significantly enhance the antibacterial activities of cellulose/PANI-based nanocomposites.[99,101–103] Likewise, a composite composed of PPY (cellulose nanopaper/chitosan/PPY: 1 inch x1 inch) demonstrated a bacterial reduction of 95.59% against *E. coli* and 99.28% against *S. aureus*.[97] It is suggested that the antibacterial efficacy of conductive composites may increase at higher concentrations (e.g.,100 mg).[98] The antimicrobial properties of conductive polymer composites can be attributed to either (a) the release of acidic dopant ions from the conducting polymers, which interact with the bacterial cell wall and/or membrane, leading to its destruction and subsequent death, or (b) the electrostatic adhesion between the bacteria and conductive polymers, facilitated by their opposite charges, which results in the rupture of the bacterial cell wall and/or membrane and ultimately causing death.[94,96,98,100]

3. Conclusion

In this study, it was demonstrated that the synthesis of PANI and PPY within CFs, made from low-quality cotton, through a chemical oxidative polymerization process yields highly versatile conductive polymer@CF composites. The amount of conductive polymers within CF was increased by repeatedly loading ANI and PY monomers into CF structures and then conducting in situ oxidative polymerization cycles. The resulting conductive polymer-containing composites exhibited excellent thermal stability compared to pure cellulose due to interactions between PANI and PPY chains with cellulose molecules. Multiple cycles of ANI loading/polymerization led to decreased CA values for PANI@CF composites, while multiple PY loading/polymerization cycles resulted in increased CA values for PPY@CF composites. The decrease in CA values of PANI@CF could be attributed to the conversion of PANI structures formed in the previous polymerization process into the emeraldine salt form induced by the presence of HCl. Conversely, the increase in CA of PPY@CF could be ascribed to the heightened amount of in situ synthesized PPY within CFs. The electrical conductivity of the PANI@CF and PPY@CF composites also increased with the multiple cycles of monomer loading/polymerization. The highest electrical conductivity was attained for 3PANI@CF and 3PPY@CF composites and was calculated to be 3.3K and 30K times higher than the conductivity of neat CF, respectively. Additionally, it was found that PANI@CF composites were very hemolytic at 1 mg mL^{-1} concentration, resulting in damage to red blood cells. In contrast, PPY@CF composites at the same concentration showed no hemolytic activity and did not cause damage to red blood cells. Moreover, the cytotoxicity of the conductive polymer@CF composites was evaluated on L929 fibroblast cells, demonstrating that at a concentration of 1 mg, the PPY@CF composites exhibited greater biocompatibility compared to PANI@CF composites. In addition, 3PPY@CF composites displayed notable antibacterial properties against both gram-negative and gram-positive bacteria, including *E. coli* and *S. aureus*, as well as against the fungus *C. albicans*.

Cellulose, with special attributes of high purity, crystallinity, strong mechanical properties, and biocompatibility, has expanded its usage beyond its traditional application in the food and beverage industry. Electroactive cellulose films hold great potential as adaptable functional materials suitable for many biomedical applications. The results of this study demonstrate the use of cellulose based conductive polymer composites for a wide range of potential applications in biotechnological domains.

4. Experimental Section

Materials: Extra pure DMAc (N, N-Dimethylacetamide, 99%, A0403006) and anhydrous LiCl (Lithium chloride, 99%, A0386841) were purchased from Acros Organics (NJ, USA). Glycerol (202 397, certified ACS) was purchased from Fisher Scientific (MA, USA). Low-quality cotton was collected from the Fiber and Biopolymer Research Institute (FBRI, Texas Tech University Lubbock, TX, USA). Ammonium persulfate (APS, 98%, Sigma-Aldrich) was employed as an oxidation agent in hydrochloric acid (HCl, 36%–38%, Sigma Aldrich) for the oxidative polymerization of aniline (ANI, 98%, Sigma Aldrich) for the in situ production of conductive polymer within CFs. Also, pyrrole (PY, 98%, Aldrich) was used as received for the synthesis of poly(pyrrole) (PPY). Iron (III) chloride anhydrous ($FeCl_3$, 99%, Acros) solution in water was employed as an initiating system. Diiodomethane (99%, Alfa Aesar) was used for SFE calculations. In the cytotoxicity analysis, L929 fibroblast cells (Mouse C3 and connective tissue) were obtained from SAP Institute, Ankara, Turkey. Trypsin (0.25%, EDTA 0.02% in PBS), Dulbecco's Modified Eagle's Medium (DMEM, with 4.5 g L^{-1} glucose, 3.7 g L^{-1} sodium pyruvate, L-Glutamine 0.5 g mL^{-1}), fetal bovine serum (FBS, heat-inactivated), and penicillin/streptomycin (10000 U mL^{-1} penicillin, 10 mg mL^{-1} streptomycin) were products of Pan Biotech GmbH. Dimethyl sulfoxide (DMSO, 99.9%, Carlo Erba), trypan blue (0.5% solution, Biological Industries), and 3-(4,5-dimethylthiazol-2-yl)−2,5-diphenyltetrazolium bromide (MTT agent, BioFroxx) were used as received. Gram-negative bacteria *Escherichia coli* ((*E. coli*, ATCC8739), Gram-positive bacteria *Staphylococcus aureus* (*S. aureus*, ATCC6538), and yeast *Candida albicans* (*C. albicans*, ATCC10231) were acquired from KWIK-STIK Microbiologics (St. Cloud, Minnesota, USA) for antibacterial activity tests. Nutrient agar (NA, Difco), and potato dextrose agar (Difco) as solid growth media and nutrient broth (NB, RPI, Merck, Darmstadt, Germany) as a liquid medium were used as received.

Purification of Cotton Fibers: Raw cotton (micronaire = 2.4) was cleaned three times using a Microdust and Trash Monitor (MTM). Then, cotton fibers were scoured and bleached in order to obtain purified cotton cellulose. For the scouring process, cotton fibers were boiled in an alkaline scouring solution (liquor ratio 1:10) containing a non-ionic wetting agent-Triton-X 100 (1 g L^{-1}) and high concentration of NaOH (8 g L^{-1}) at 90 °C for 1 h. After that, the solution was poured off and cotton was rinsed with fresh water. The scoured fibers were boiled in a bleaching solution (liquor ratio 1:10) containing wetting agent – Triton-X 100 (0.25 g L^{-1}), NaOH (0.35 g L^{-1}), sodium silicate (3 g L^{-1}), sodium carbonate (0.7 g L^{-1}), and sodium hypochlorite (6 g L^{-1}) at 90 °C for 90 min. Purified cotton fibers were then boiled in fresh water at 90 °C for 20 min and neutralized with 0.25 g L^{-1} acetic acid. Finally, the purified cotton was air-dried for the next use. The air-dried cotton fibers were opened twice using the Microdust and Trash Monitor (MTM).

Dissolution of Cotton Fibers and Cellulose Film Preparation: Scoured and bleached cotton fibers were dissolved in DMAc/LiCl solvent system. Initially, oven-dried cotton fibers (105 °C, 24 h) were added to a hot DMAc solution at 80 °C (1% w:v) and stirred for 30 min. Subsequently, oven dried LiCl (8% w: v) was added to the solution, and stirring was continued for another 3 h at 80 °C. Following that, the temperature was lowered to 50 °C, and the dissolution was carried out overnight. Afterward, the solution was transferred to an oven (105 °C) for 12 h. Then, the solution was taken out of the oven and allowed to reach room temperature. Cellulose solution was poured into glass molds and left inside a fume hood for 24 h. Deionized (DI) water was used to regenerate the gelated films for five days. After two days of plasticization with a 30% aqueous glycerol (w:v) solution, the regenerated cellulose films were hot-pressed for 15 min at 120 °C.

In Situ Conductive Polymer Synthesis Within Cellulose Films: For the preparation of conductive polymer containing cellulose films as composites, a previous protocol from this research group was followed with some modifications.[46,70] For this purpose, the cellulose films (CFs) were cut into several pieces with a size of 1.5 × 1.5 cm, and each piece was placed into 5 mL of aniline (ANI) and pyrrole (PY), separately, and stirred at 250 rpm for 12 h to load the relevant monomers into CFs. Then, the ANI and PY loaded CFs were polymerized in situ as conductive polymer@CF composites, as given below.

Preparation of PANI@CF Composites: The ANI loaded CF pieces were placed into 10 mL of DI water and decanted after stirring for 1 min to remove un-adsorbed ANI molecules, and this washing procedure was repeated three times. Next, 20 mL of solutions of APS in 1 M HCl were freshly prepared by dissolving 1 g of APS in 20 mL 1 M HCl solution, and the ANI loaded CF pieces were placed into these solutions separately. The in situ polymerization reactions of ANI monomers within CF pieces were carried out for 12 h under constant stirring at 250 rpm at room temperature. Finally, the prepared 1PANI@CF composites were separated from the solution via decantation of supernatant and were washed via stirring in 10 mL of fresh DI water (x3), and ethanol (x1) each for

1 min. The washed 1PANI@CF composites were dried in an oven at 50 °C, and the ANI monomer loading/polymerization step was employed two more times to prepare 2PANI@CF, and 3PANI@CF composites. The prepared 1PANI@CF, 2PANI@CF, and 3PANI@CF composites were stored in closed tubes for characterization and further use.

Preparation of PPY@CF Composites: First, the CF pieces loaded with PY were rinsed according to the previously described method to eliminate any remaining unloaded PY monomers from the CFs, repeating the process three times with DI water. Subsequently, each PY-loaded CF piece was submerged in freshly prepared 20 mL of 0.5 M $FeCl_3$ solution and stirred at 250 rpm for 12 h at room temperature to facilitate the in situ polymerization of the loaded PY monomers within the CFs. The prepared 1PPY@CF composites were then separated from the supernatant and washed using the same process mentioned above. Similarly, the washed and dried 1PPY@CF composites were used to prepare 2PPY@CF and 3PPY@CF composites through repeated cycles of PY monomer loading and polymerization, as detailed above. These composites, 1PPY@CF, 2PPY@CF, and 3PPY@CF were stored in sealed containers for subsequent use.

Biomedical Properties of PANI@CF and PPY@CF Composites: The details of the biomedical properties of conductive polymer containing CF composites were evaluated via hemocompatibility, biocompatibility, and antimicrobial assays, and the relevant details were provided in Supporting Information.

Supporting Information

Supporting Information is available from the Wiley Online Library or from the author.

Acknowledgements

The startup fund through the University of South Florida, Ophthalmology department was greatly appreciated.

Conflict of Interest

The authors declare no conflict of interest.

Data Availability Statement

Data sharing is not applicable to this article as no new data were created or analyzed in this study.

Keywords

antimicrobial cellulose composite, cellulose-conductive polymer composite, conductive cellulose, cotton derived cellulose films

Received: July 5, 2024
Revised: August 28, 2024
Published online: September 10, 2024

[1] J. Wang, L. Wang, D. J. Gardner, S. M. Shaler, Z. Cai, *Cellulose* **2021**, *28*, 4511.
[2] P. Khamwongsa, P. Wongjom, H. Cheng, C. C. Lin, S. ;Ummartyotin, *Compos. Part C Open Access* **2022**, *9*, 100314.
[3] C. Chen, Y. Kuang, S. Zhu, I. Burgert, T. Keplinger, A. Gong, T. Li, L. Berglund, S. J. Eichhorn, L. Hu, *Nat. Rev. Mater.* **2020**, *5*, 642.
[4] X. Du, Z. Zhang, W. Liu, Y. Deng, *Nano Energy* **2017**, *35*, 299.
[5] X. Liu, W. Xiao, X. Ma, L. Huang, Y. Ni, L. Chen, X. Ouyang, J. Li, *Carbohydr. Polym.* **2020**, *250*, 116969.
[6] S. C. Rodrigues, M. Andrade, J. Moffat, F. D. Magalhães, A. Mendes, *J. Memb. Sci.* **2019**, *572*, 390.
[7] S. Saedi, C. V. Garcia, J. T. Kim, G. H. Shin, *Cellulose* **2021**, *28*, 8877.
[8] E.-E. Tudoroiu, C.-E. Dinu-Pîrvu, M. G. Albu Kaya, L. Popa, V. Anuța, R. M. Prisada, M. V. Ghica, *Pharmaceuticals* **2021**, *14*, 1215.
[9] T. Aditya, J. P. Allain, C. Jaramillo, A. M. Restrepo, *Int. J. Mol. Sci.* **2022**, *23*, 610.
[10] M. S. Hasanin, *Starch – Stärke* **2022**, *74*, 2200060.
[11] T. Nezakati, A. Seifalian, A. Tan, A. M. Seifalian, *Chem. Rev.* **2018**, *118*, 6766.
[12] N. K., C. S. Rout, *RSC Adv.* **2021**, *11*, 5659.
[13] D. Runsewe, T. Betancourt, J. A. Irvin, *Materials (Basel)* **2019**, *12*, 2629.
[14] A. Maziz, E. Özgür, C. Bergaud, L. Uzun, *Sensors and Actuators Reports* **2021**, *3*, 100035.
[15] S. Lee, B. Ozlu, T. Eom, D. C. Martin, B. S. Shim, *Biosens. Bioelectron.* **2020**, *170*, 112620.
[16] T. Distler, A. R. Boccaccini, *Acta Biomater.* **2020**, *101*, 1.
[17] R. Balint, N. J. Cassidy, S. H. Cartmell, *Acta Biomater.* **2014**, *10*, 2341.
[18] X. Guo, A. Facchetti, *Nat. Mater.* **2020**, *19*, 922.
[19] S. Nambiar, J. T. W. Yeow, *Biosens. Bioelectron.* **2011**, *26*, 1825.
[20] K. Bednarczyk, W. Matysiak, T. Tański, H. Janeczek, E. Schab-Balcerzak, M. Libera, *Sci. Rep.* **2021**, *11*, 7487.
[21] E. N. Zare, P. Makvandi, B. Ashtari, F. Rossi, A. Motahari, G. Perale, *J. Med. Chem.* **2020**, *63*, 1.
[22] M. Beygisangchin, S. Abdul Rashid, S. Shafie, A. R. Sadrolhosseini, H. N. Lim, *Polymers (Basel)* **2021**, *13*, 2003.
[23] T. Samwang, N. M. Watanabe, Y. Okamoto, S. Srinives, H. Umakoshi, *ACS Omega* **2023**, *8*, 48946.
[24] S. Kim, L. K. Jang, H. S. Park, J. Y. Lee, *Sci. Rep.* **2016**, *6*, 30475.
[25] D. . Ateh, H. . Navsaria, P. Vadgama, *J. R. Soc. Interface* **2006**, *3*, 741.
[26] R. Kumar, J. Travas-Sejdic, L. P. Padhye, *Chem. Eng. J. Adv.* **2020**, *4*, 100047.
[27] R. J. Racicot, R. L. Clark, H.-B. Liu, S. C. Yang, M. N. Alias, R. Brown, *MRS Proc* **1995**, *413*, 529.
[28] J. Kim, J. Lee, J. You, M.-S. Park, M. S. Al Hossain, Y. Yamauchi, J. H. Kim, *Mater. Horiz.* **2016**, *3*, 517.
[29] Y. Wang, A. Liu, Y. Han, T. Li, *Polym. Int.* **2020**, *69*, 7.
[30] Y. Feng, X. Zhang, Y. Shen, K. Yoshino, W. Feng, *Carbohydr. Polym.* **2012**, *87*, 644.
[31] A. N. Aleshin, A. S. Berestennikov, P. S. Krylov, I. P. Shcherbakov, V. N. Petrov, I. N. Trapeznikova, R. I. Mamalimov, A. K. Khripunov, A. A. Tkachenko, *Synth. Met.* **2015**, *199*, 147.
[32] W. Hu, S. Chen, Z. Yang, L. Liu, H. Wang, *J. Phys. Chem. B* **2011**, *115*, 8453.
[33] S. S. Rumi, S. Liyanage, N. Abidi, *Cellulose* **2021**, *28*, 2021.
[34] C.-G. Wu, H. O. Marcy, D. C. DeGroot, J. L. Schindler, C. R. Kannewurf, M. G. Kanatzidis, *Synth. Met.* **1991**, *41*, 693.
[35] D. K. Moon, J.-Y. Yun, K. Osakada, T. Kambara, T. Yamamoto, *Mol. Cryst. Liq. Cryst.* **2007**, *464*, 177.
[36] A. K. Sharma, P. Bhardwaj, S. Kumar Dhawan, Y. Sharma, *Adv. Mater. Lett.* **2015**, *6*, 414.
[37] S.-J. Tang, A.-T. Wang, S.-Y. Lin, K.-Y. Huang, C.-C. Yang, J.-M. Yeh, K.-C. Chiu, *Polym. J.* **2011**, *43*, 667.
[38] D. Beneventi, S. Alila, S. Boufi, D. Chaussy, P. Nortier, *Cellulose* **2006**, *13*, 725.
[39] N. Ballav, M. Biswas, *Polym. J.* **2004**, *36*, 162.
[40] M. Grzybowski, B. Sadowski, H. Butenschön, D. T. Gryko, *Angew. Chem., Int. Ed.* **2020**, *59*, 2998.
[41] X. Peng, J. Zhao, G. Ma, Y. Wu, S. Hu, Z. Ruan, P. Feng, *Green Chem.* **2021**, *23*, 8853.

[42] Y. Tan, K. Ghandi, *Synth. Met.* **2013**, *175*, 183.
[43] S. M. Ahmed, *Polym. Degrad. Stab.* **2004**, *85*, 605.
[44] A. John, S. K. Mahadeva, J. Kim, *Smart Mater. Struct.* **2010**, *19*, 10.
[45] Z. Ahmad, M. A. Choudhary, A. Mehmood, R. Wakeel, T. Akhtar, M. A. Rafiq, *Macromol. Res.* **2016**, *24*, 596.
[46] N. Sahiner, S. Demirci, *Synth. Met.* **2017**, *227*, 11.
[47] J. Stejskal, M. Trchová, I. Sapurina, *J. Appl. Polym. Sci.* **2005**, *98*, 2347.
[48] H.-J. Lee, T.-J. Chung, H.-J. Kwon, H.-J. Kim, W. T. Y. Tze, *Cellulose* **2012**, *19*, 1251.
[49] X. Zhang, J. Zhu, N. Haldolaarachchige, J. Ryu, D. P. Young, S. Wei, *Z. Guo* **2012**, *53*, 2109.
[50] R. L. Razalli, M. M. Abdi, P. M. Tahir, A. Moradbak, Y. Sulaiman, L. Y. Heng, *RSC Adv.* **2017**, *7*, 25191.
[51] M. J. Liu, K. Tzou, R. V. Gregory, *Synth. Met.* **1994**, *63*, 67.
[52] T. V. Shishkanova, I. Sapurina, J. Stejskal, V. Král, R. Volf, *Anal. Chim. Acta* **2005**, *553*, 160.
[53] Z. Zhang, Z. Wei, M. Wan, *Macromolecules* **2002**, *35*, 5937.
[54] N. V. Blinova, J. Stejskal, M. Trchová, J. Prokeš, *Polym. Int.* **2008**, *57*, 66.
[55] H. Ha, S. Müller, R. P. Baumann, B. Hwang, *Facta Univ. Ser. Mech. Eng.* **2024**, *22*, 1.
[56] S. G. Gizer, V. R. Bhethanabotla, R. S. Ayyala, N. Sahiner, *Surfaces and Interfaces* **2023**, *37*, 102646.
[57] X. Yu, S. M. Hörst, C. He, P. McGuiggan, K. Kristiansen, X. Zhang, *Astrophys. J.* **2020**, *905*, 88.
[58] S. A. Fraser, W. E. van Zyl, *RSC Adv.* **2022**, *12*, 22031.
[59] G. Nyström, A. Mihranyan, A. Razaq, T. Lindström, L. Nyholm, M. Strømme, *J. Phys. Chem. B* **2010**, *114*, 4178.
[60] S. K. Pramanik, H. Suzuki, *ACS Appl. Mater. Interfaces* **2020**, *12*, 37741.
[61] X. Tan, C. Hu, X. Li, H. Liu, J. Qu, *J. Memb. Sci.* **2020**, *605*, 118088.
[62] L. Xu, W. Chen, A. Mulchandani, Y. Yan, *Angew. Chem. – Int. Ed.* **2005**, *44*, 6009.
[63] M. Liu, F.-Q. Nie, Z. Wei, Y. Song, L. Jiang, *Langmuir* **2010**, *26*, 3993.
[64] M. M. Menamparambath, *ACS Mater. Au* **2024**, *4*, 115.
[65] T. Darmanin, F. Guittard, *Prog. Polym. Sci.* **2014**, *39*, 656.
[66] D. Liu, C. Huyan, Z. Wang, Z. Guo, X. Zhang, H. Torun, D. Mulvihill, B. Bin Xu, F. Chen, *Mater. Horiz.* **2023**, *10*, 2800.
[67] S. Sharma, P. Sudhakara, A. A. B. Omran, J. Singh, R. A. Ilyas, *Polymers* **2021**, *13*, 2898.
[68] K. Lota, V. Khomenko, E. Frackowiak, *J. Phys. Chem. Solids* **2004**, *65*, 295.
[69] S. Suematsu, Y. Oura, H. Tsujimoto, H. Kanno, K. Naoi, *Electrochim. Acta* **2000**, *45*, 3813.
[70] N. Sahiner, S. Demirci, *React. Funct. Polym.* **2016**, *105*, 60.
[71] A. H. Majeed, L. A. Mohammed, O. G. Hammoodi, S. Sehgal, M. A. Alheety, K. K. Saxena, S. A. Dadoosh, I. K. Mohammed, M. M. Jasim, N. U. Salmaan, *Int. J. Polym. Sci.* **2022**, 9047554, 1.
[72] A. Mahun, S. Abbrent, P. Bober, J. Brus, L. Kobera, *Synth. Met.* **2020**, *259*, 116250.
[73] S. Demirci, S. D. Sutekin, N. Sahiner, *J. Compos. Sci.* **2020**, *4*, 33.
[74] M. Parit, H. Du, X. Zhang, C. Prather, M. Adams, Z. Jiang, *Carbohydr. Polym.* **2020**, *240*, 116304.
[75] H. Kim, J.-Y. Yi, B.-G. Kim, J. E. Song, H.-J. Jeong, H. R. Kim, *PLoS One* **2020**, *15*, e0233952.
[76] E. Alonso, M. Faria, F. Mohammadkazemi, M. Resnik, A. Ferreira, N. Cordeiro, *Carbohydr. Polym.* **2018**, *183*, 254.
[77] M. Huang, Y. Tang, X. Wang, P. Zhu, T. Chen, Y. Zhou, *Prog. Org. Coatings* **2021**, *159*, 106452.
[78] R. Luna-Vázquez-Gómez, M. E. Arellano-García, J. C. García-Ramos, P. Radilla-Chávez, D. S. Salas-Vargas, F. Casillas-Figueroa, B. Ruiz-Ruiz, N. Bogdanchikova, A. Pestryakov, *Materials* **2021**, *14*, 2792.
[79] S. O. Sowemimo-Coker, *Transfus. Med. Rev.* **2002**, *16*, 46.
[80] X. Wang, X. Gu, C. Yuan, S. Chen, P. Zhang, T. Zhang, J. Yao, F. Chen, G. Chen, *J. Biomed. Mater. Res. Part A* **2004**, *68A*, 411.
[81] Y. O. Mezhuev, A. A. Artyukhov, A. I. Piskareva, M. I. Shtil'man, M. M. Gol'din, Y. V. Korshak, I. V. Solov'eva, A. K. Evseev, *Russ. J. Appl. Chem.* **2015**, *88*, 1026.
[82] J. López-García, M. Lehocký, P. Humpolíček, P. Sáha, *J. Funct. Biomater.* **2014**, *5*, 43.
[83] M.-R. Chia, S.-W. Phang, I. Ahmad, *Polymers* **2022**, *14*, 5168.
[84] P. Humpolíček, V. Kašpárková, J. Pacherník, J. Stejskal, P. Bober, Z. Capáková, K. A. Radaszkiewicz, I. Junkar, M. Lehocký, *Mater. Sci. Eng. C* **2018**, *91*, 303.
[85] Y. Zhang, M. Zhou, C. Dou, G. Ma, Y. Wang, N. Feng, W. Wang, L. Fang, *J. Bioact. Compat. Polym.* **2019**, *34*, 16.
[86] B. Guo, J. Zhao, C. Wu, Y. Zheng, C. Ye, M. Huang, S. Wang, *Colloids Surf., B* **2019**, *177*, 346.
[87] A. Vaitkuviene, V. Kaseta, J. Voronovic, G. Ramanauskaite, G. Biziuleviciene, A. Ramanaviciene, A. Ramanavicius, *J. Hazard. Mater.* **2013**, *250*, 167.
[88] Y. Liu, S. Ahmed, D. E. Sameen, Y. Wang, R. Lu, J. Dai, S. Li, W. Qin, *Trends Food Sci. Technol.* **2021**, *112*, 532.
[89] N. Asim, M. Badiei, M. Mohammad, *Emergent Mater* **2022**, *5*, 703.
[90] J. S. Yaradoddi, N. R. Banapurmath, S. V. Ganachari, M. E. M. Soudagar, N. M. Mubarak, S. Hallad, S. Hugar, H. Fayaz, *Sci. Rep.* **2020**, *10*, 21960.
[91] A. C. M. Cidreira, K. C. de Castro, T. Hatami, L. Z. Linan, L. H. I. Mei, *Biomed. Microdevices* **2021**, *23*, 43.
[92] V. Kanikireddy, K. Varaprasad, T. Jayaramudu, C. Karthikeyan, R. Sadiku, *Int. J. Biol. Macromol.* **2020**, *164*, 963.
[93] L. Zheng, S. Li, J. Luo, X. Wang, *Front. Bioeng. Biotechnol.* **2020**, *8*.
[94] J. George, S. S N, *Nanotechnol. Sci. Appl.* **2015**, *8*, 45.
[95] M. S. Hasanin, A. M. Mostafa, E. A. Mwafy, O. M. Darwesh, *Environ. Nanotechnology, Monit. Manag.* **2018**, *10*, 409.
[96] A. B. Abou Hammad, M. E. Abd El-Aziz, M. S. Hasanin, S. Kamel, *Carbohydr. Polym.* **2019**, *216*, 54.
[97] H. Du, M. Parit, K. Liu, M. Zhang, Z. Jiang, T.-S. Huang, X. Zhang, C. Si, *ACS Appl. Mater. Interfaces* **2021**, *13*, 32115.
[98] B. Bideau, J. Bras, S. Saini, C. Daneault, E. Loranger, *Mater. Sci. Eng. C* **2016**, *69*, 977.
[99] A. Shalini, R. Nishanthi, P. Palani, V. Jaisankar, *Mater. Today Proc* **2016**, *3*, 1633.
[100] M. Maruthapandi, A. Saravanan, A. Gupta, J. H. T. Luong, A. Gedanken, *Macromol* **2022**, *2*, 78.
[101] A. K. Rana, F. Scarpa, V. K. Thakur, *Ind. Crops Prod.* **2022**, *187*, 115356.
[102] R. A. Hamouda, R. R. Makharita, F. A. K. Qarabai, F. S. Shahabuddin, A. A. Saddiq, L. A. Bahammam, S. W. El-Far, M. A. Bukhari, M. A. Elaidarous, A. Abdella, *Microorganisms* **2024**, *12*, 1.
[103] R. J. B. Pinto, S. Daina, P. Sadocco, C. P. Neto, T. Trindade, *Biomed Res. Int.* **2013**, 280512.

